

See discussions, stats, and author profiles for this publication at: <https://www.researchgate.net/publication/279301365>

Terahertz Spectroscopy and Solid-State Density Functional Theory Calculations of Cyanobenzaldehyde Isomers

ARTICLE in THE JOURNAL OF PHYSICAL CHEMISTRY A · JUNE 2015

Impact Factor: 2.69 · DOI: 10.1021/acs.jpca.5b01942 · Source: PubMed

READS

32

9 AUTHORS, INCLUDING:



Shaumik Ray

Council of Scientific and Industrial Research (...)

10 PUBLICATIONS 4 CITATIONS

SEE PROFILE



Kathirvel Nallappan

Polytechnique Montréal

7 PUBLICATIONS 6 CITATIONS

SEE PROFILE



Vaibhav Kaware

CSIR - National Chemical Laboratory, Pune

13 PUBLICATIONS 13 CITATIONS

SEE PROFILE



Kavita Joshi

CSIR - National Chemical Laboratory, Pune

33 PUBLICATIONS 473 CITATIONS

SEE PROFILE

Terahertz Spectroscopy and Solid-State Density Functional Theory Calculations of Cyanobenzaldehyde Isomers

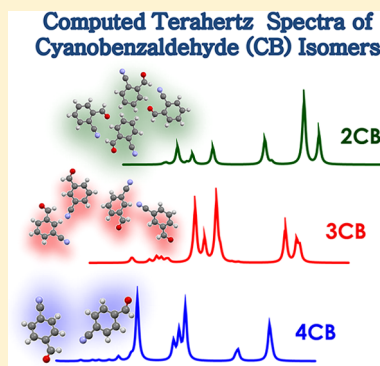
Jyotirmayee Dash,^{†,§} Shaumik Ray,^{†,§} Kathirvel Nallappan,[†] Vaibhav Kaware,[‡] Nitin Basutkar,[‡] Rajesh G. Gonnade,[‡] Ashootosh V. Ambade,[‡] Kavita Joshi,[‡] and Bala Pesala^{*,†,§}

[†]CSIR-Central Electronics Engineering Research Institute, CSIR Madras Complex, Chennai, India 600113

[‡]CSIR-National Chemical Laboratory, Pune, India 411008

[§]Academy of Scientific and Innovative Research, CSIR-SERC, Chennai, India 600113

ABSTRACT: Spectral signatures in the terahertz (THz) frequency region are mainly due to bulk vibrations of the molecules. These resonances are highly sensitive to the relative position of atoms in a molecule as well as the crystal packing arrangement. To understand the variation of THz resonances, THz spectra (2–10 THz) of three structural isomers: 2-, 3-, and 4-cyanobenzaldehyde have been studied. THz spectra obtained from Fourier transform infrared (FTIR) spectrometry of these isomers show that the resonances are distinctly different especially below 5 THz. For understanding the intermolecular interactions due to hydrogen bonds, four molecule cluster simulations of each of the isomers have been carried out using the B3LYP density functional with the 6-31G(d,p) basis set in Gaussian09 software and the compliance constants are obtained. However, to understand the exact reason behind the observed resonances, simulation of each isomer considering the full crystal structure is essential. The crystal structure of each isomer has been determined using X-ray diffraction (XRD) analysis for carrying out crystal structure simulations. Density functional theory (DFT) simulations using CRYSTAL14 software, utilizing the hybrid density functional B3LYP, have been carried out to understand the vibrational modes. The bond lengths and bond angles from the optimized structures are compared with the XRD results in terms of root-mean-square-deviation (RMSD) values. Very low RMSD values confirm the overall accuracy of the results. The simulations are able to predict most of the spectral features exhibited by the isomers. The results show that low frequency modes (<3 THz) are mediated through hydrogen bonds and are dominated by intermolecular vibrations.



1. INTRODUCTION

Over the last couple of decades, terahertz (THz) spectroscopy (0.1–10 THz) has become increasingly popular due to its non-invasive and nondestructive means of acquiring spectral fingerprints. This technique has been successfully applied in various applications including counterfeit detection of pharmaceutical drugs and identification of explosives and biological molecules.^{1–3}

The resonances of individual vibrational modes arise from the reduced mass and the potential forces of the system.⁴ The weaker the force constant and larger the reduced mass, the lower are the vibrational frequencies. Hence, intramolecular stretching, twisting, and bending vibrations typically arise in the near-infrared (NIR)/mid-infrared (MIR) region whereas low frequency bulk vibrations and intermolecular vibrations fall in the THz region. The THz region, especially 0.1–5 THz, provides valuable information on various vibrational modes: intermolecular vibrational modes, torsional vibrations, and hydrogen bond stretches in many chemical and biological compounds.⁵

Recent THz spectroscopy studies show that it is an efficient technique to identify and analyze the low frequency vibrational modes in various biological molecules, including DNA components and proteins.^{6,7} THz spectroscopy of DNA components⁶ shows that the resonances are mainly due to intermolecular

vibrational modes. Study of THz vibrational modes of proteins⁷ confirm the origin of lower THz resonances as bulk vibrations that can be used for identification of structural conformation of the molecule. Study of isomers provides a good model system to better understand the effect of change in bulk structure as well as relative arrangement of atoms on the THz vibrational modes.

Several isomers of organic molecules have been studied earlier using THz spectroscopy such as studies on the two isomers of dicyanobenzene⁸ show that the spectra from 20 to 100 cm⁻¹ (0.6–3 THz) are mainly dominated by intermolecular rotations. THz resonances are distinctly different in the low frequency region due to the difference in the crystal packing arrangement of the isomers. Study of benzoic acid isomers⁴ in the spectral region 18–150 cm⁻¹ (0.54–4.5 THz) shows that the THz resonances are mainly due to the combined effect of intramolecular and intermolecular vibrational modes and hence are highly sensitive to the structure of the isomers. THz spectroscopy has also been used to distinguish similarly structured molecules with amide groups including benzamide, acrylamide, caprolactam, salicylamide, and sulfanilamide,⁹ where the spectra have been compared

Received: February 27, 2015

Revised: June 16, 2015

with the vibrational modes obtained using DFT simulations. The five molecules exhibit distinct frequency bands in the region 0.2–2.6 THz, which are related to torsion, rocking, and wagging modes. These earlier studies give an insight into understanding and analyzing the origin of THz resonances of various organic isomers.

Cyanobenzaldehyde is an interesting molecule to study and understand the resonances in the THz region, especially intermolecular vibrations mediated through hydrogen bonds. In this paper, cyanobenzaldehyde isomers are studied to understand how minor variation in the positions of atoms in an organic molecule and different crystalline arrangements result in a change of THz resonance frequencies.

THz spectra of the isomers obtained by FTIR spectroscopy show distinct resonances. To understand the origin of resonances, initially DFT simulations have been carried out by considering a single molecule of each isomer using B3LYP density functional with 6-31G(d,p) basis set in Gaussian09 software.¹⁰ The simulation results match well with the experimental results at higher frequencies (>5 THz), as these resonances are due to intramolecular vibrations. However, single molecule simulations cannot predict the vibrational modes originating from intermolecular vibrations. To understand the origin of the THz resonances at lower frequencies, especially below 3 THz, full crystal structure simulations have been carried out using CRYSTAL14^{11,12} software. The simulation results clearly explain the origin of low frequency THz resonances and factors contributing to the shift in resonances due to the change in position of functional groups. In spite of the structural similarity, individual molecules show distinct fingerprints in the THz region, which can be used for their chemical recognition.

Furthermore, the understanding gained from this study can be used to design and engineer organic molecules, which can show sharp and distinct resonances in the THz region (especially below 3 THz).¹³

2. THZ SPECTROSCOPY RESULTS

2-Cyanobenzaldehyde (97% pure), 3-cyanobenzaldehyde (98% pure), and 4-cyanobenzaldehyde (98% pure) samples have been purchased from Avra Synthesis Pvt. Ltd. and are used without further purification. High density polyethylene (HDPE) has been mixed with the sample in the ratio of roughly 10:90 by concentration. Smooth pellets of 1 mm thickness were prepared after applying a pressure of 15 tonnes in a potassium bromide (KBr) press unit for 2 min. The samples have been scanned in a Nicolet 6700, Thermo Scientific FTIR instrument capable of taking Far-Infrared (FIR) measurements over a wide frequency range (2 THz to 10 THz). Measurements are carried out with a resolution of 4 cm⁻¹ and the spectrum obtained is an average of 136 scans.

Figure 1 compares the THz spectra of the three cyanobenzaldehyde isomers obtained from the experimental results. The absorbance values are normalized to one for comparison purposes. The experimental results clearly show distinct resonances for each of the isomer especially in the lower THz frequency range (<5 THz). To understand the origin of the THz resonances and how the change in the position of –CN group affects the resonances, DFT simulations have been carried out. To understand low frequency vibrational modes, which are mainly due to intermolecular vibrational modes, simulations by considering the full crystal structure are essential. For this purpose, the exact crystal structure has to be determined, which has been obtained using X-ray diffraction (XRD) analysis.

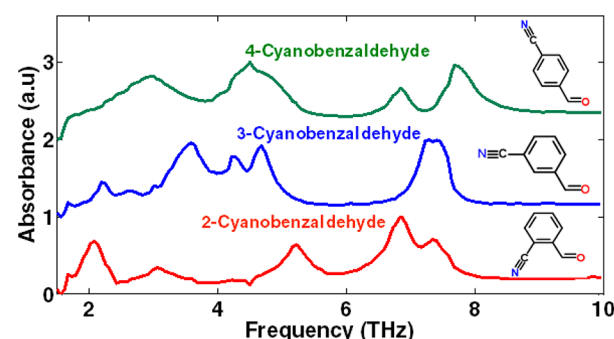


Figure 1. THz spectra of cyanobenzaldehyde isomers.

3. CRYSTAL STRUCTURE DETERMINATION USING XRD TECHNIQUE

Single-crystal X-ray intensity measurements of 2-, 3-, and 4-cyanobenzaldehyde were recorded using a Bruker SMART APEX II single crystal X-ray CCD diffractometer at 100 (2) K, with graphite-monochromatized (Mo K α = 0.71073 Å) radiation. The X-ray generator was operated at 50 kV and 30 mA. Diffraction data were collected with a ω scan width of 0.5° at different settings of φ and 2θ . The sample to detector distance was fixed at 5 cm. The X-ray data acquisition was monitored by APEX II program.¹⁴

All the data were corrected for Lorentz-polarization and absorption effects using SAINT and SADABS programs integrated in APEX II program package.¹⁴ The structures were solved by direct method and refined by full matrix least-squares, based on F2, using SHELX-97.¹⁵ All the hydrogen atoms were placed in geometrically idealized position and constrained to ride on their parent atoms. Figure 2 shows the arrangements of closely associated molecules through C–H \cdots N and C–H \cdots O hydrogen bonding interactions in the unit cells of respective cyanobenzaldehyde isomers.

Crystal structures of 2-cyanobenzaldehyde, 3-cyanobenzaldehyde and 4-cyanobenzaldehyde belong to monoclinic space group $P2_1/c$, orthorhombic chiral group $P2_12_12_1$, and monoclinic noncentrosymmetric space group Pc , respectively. The asymmetric unit of all the isomers contained one molecule. The labeling schemes of all the isomers are given in Figure 3. Crystallographic data of all the isomers are given in Table 1, and the geometrical parameters of intermolecular interactions of 2-, 3-, and 4-cyanobenzaldehyde are given in Table 2. Bond lengths from XRD analysis for 2-cyanobenzaldehyde, 3-cyanobenzaldehyde, and 4-cyanobenzaldehyde are given in Tables 4, 6, and 8, respectively.

4. DFT SIMULATIONS

DFT simulations of each isomer have been carried out using Gaussian09 software by considering single molecule with full geometry optimizations. Vibrational frequency calculations are performed on the optimized structures. Similarly, full crystal structure simulations have been carried out using CRYSTAL14 software to understand the low frequency vibrational modes.

4.1. Simulations Using Gaussian09. Initially, Gaussian09 simulation software has been used for frequency calculations by considering single molecule of each isomer. DFT method with hybrid functional Becke–3–Lee–Yang–Parr (B3LYP) and double- ζ polarized basis set with six d-type Cartesian–Gaussian polarization functions (6-31G(d,p))¹⁶ has been employed for the simulations. The energy convergence criterion for both

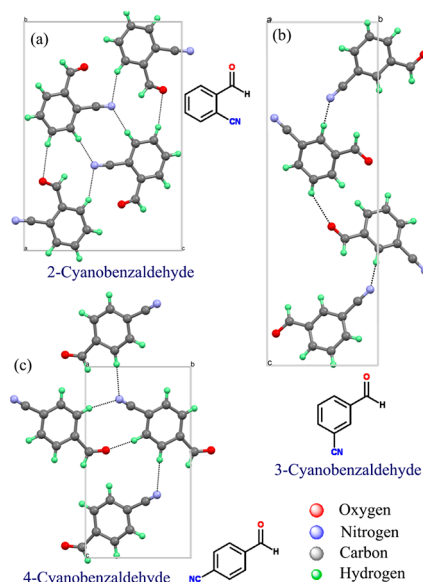


Figure 2. Representation of the crystalline unit cells displaying molecular arrangement in (a) 2-cyanobenzaldehyde, (b) 3-cyanobenzaldehyde, and (c) 4-cyanobenzaldehyde.

optimization and vibrational frequency calculation is set to 10^{-8} hartree. Figure 4 shows the comparison between experimental results and Gaussian simulation results of each isomer.

As seen in Figure 4, the simulation results match fairly well at higher frequencies (>5 THz). This is because higher resonances are mainly due to intramolecular vibrations. However, Gaussian simulation results are not able to predict the lower THz frequencies especially below 3 THz because intermolecular bond vibrations cause the resonances in this region. For accurate prediction of the resonances especially at lower THz frequencies, full crystal simulations need to be carried out, where both intermolecular and intramolecular vibrational modes can be analyzed.

4.2. Characterizing Intermolecular Hydrogen Bond Strengths Using Compliance Constants. Lower THz resonances (<3 THz) originate due to weak intermolecular hydrogen bond interactions. Hence, the strengths of various hydrogen bonds in each of the isomers have been analyzed using compliance constant formalism.¹⁷ Compliance constants (inverse of relaxed force constants) are invariant with respect to change in the coordinate system unlike the rigid force constants¹⁸ and hence can be effectively used to compare various intermolecular interactions. A lower numerical value of the

compliance constant represents a stronger bond and a higher value represents a weaker bond.

To understand hydrogen bond interactions, four molecule cluster simulations using Gaussian09 software have been done for all the isomers. B3LYP density functional with 6-31G(d,p) basis set has been used for energy optimization and for obtaining Hessian matrix corresponding to rigid force constants. The SCF convergence criterion for the calculations is set to 10^{-11} hartree. Subsequently, compliance constants of various hydrogen bonds have been calculated by using the COMPLIANCE 3.0.2 program and are shown in Figure 5. Table 3 below summarizes the compliance constant values for all the isomers.

The compliance constant values have been calculated for C–H \cdots O and C–H \cdots N stretching modes. The compliance constants given in Table 3 show that the values for C–H \cdots O and C–H \cdots N bonds in the cyanobenzaldehyde isomers are much higher compared to the typical O–H \cdots O, N–H \cdots N, O–H \cdots N, and N–H \cdots O bonds as mentioned in the published literature.¹⁷ This shows that the C–H \cdots O and C–H \cdots N bonds are weak hydrogen bonds which result in lower THz resonances. As shown in Table 3, the compliance constants for C–H \cdots O and C–H \cdots N bonds of 2- and 3-cyanobenzaldehyde are almost equal whereas the compliance constants values for 4-cyanobenzaldehyde are comparatively higher. This shows that hydrogen bond strength of 4-cyanobenzaldehyde is comparatively less compared to 2- and 3-cyanobenzaldehyde.

4.3. Simulations Using CRYSTAL14. Crystal structure simulations are performed using B3LYP density functional in combination with the atom-centered Gaussian type 6-31G(d,p) basis sets using CRYSTAL14 software package. The crystal structure of 2-, 3-, and 4-cyanobenzaldehyde, obtained by XRD analysis has been further optimized before carrying out vibrational mode calculations. The optimization has been done by computing the analytical gradients of the energy with respect to the atomic coordinates only without changing the lattice parameters.^{11,12} Bond lengths and bond angles are determined from the optimized structures and have been compared with the XRD results using root-mean-square-deviation (RMSD) values. The RMSD values are calculated as the root-mean-square value of the deviation of simulation output (S_i) from the experimental output (E_i) as shown in (1). Vibrational frequencies are computed at the Γ point, by the diagonalization of mass-weighted Hessian matrix. The normal modes associated with each vibration are obtained from the eigenvectors of the matrix.^{11,12}

$$\text{RMSD} = \sqrt{\frac{\sum_{i=1}^n (E_i - S_i)^2}{n}} \quad (1)$$

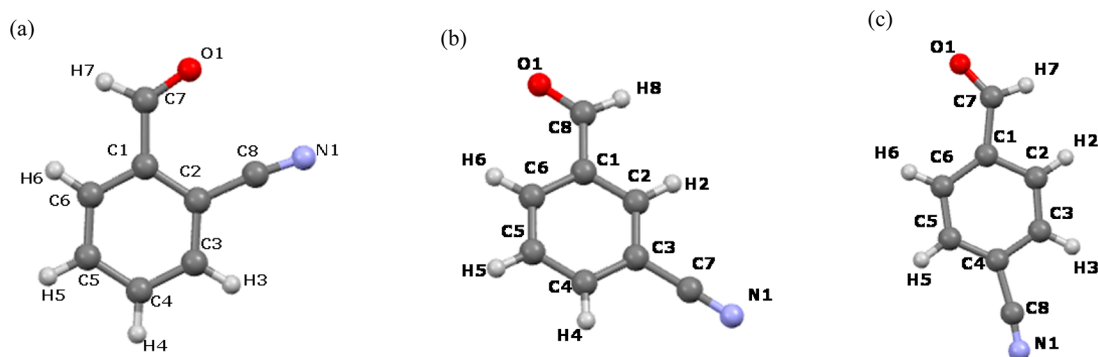


Figure 3. Ball and stick model of (a) 2-cyanobenzaldehyde, (b) 3-cyanobenzaldehyde, and (c) 4-cyanobenzaldehyde with labeling scheme.

Table 1. Crystallographic Data for 2-, 3-, and 4-Cyanobenzaldehyde

compound	2-cyanobenzaldehyde	3-cyanobenzaldehyde	4-cyanobenzaldehyde
formula	C ₈ H ₅ NO	C ₈ H ₅ NO	C ₈ H ₅ NO
<i>M_r</i>	131.13	131.13	131.13
crystal size, mm	0.54 × 0.45 × 0.39	0.76 × 0.42 × 0.15	0.49 × 0.43 × 0.32
temp (K)	100 (2)	100 (2)	100 (2)
crystal system	monoclinic	orthorhombic	monoclinic
space group	<i>P</i> 2 ₁ / <i>c</i>	<i>P</i> 2 ₁ 2 ₁ 2 ₁	<i>P</i> ₂
<i>a</i> /Å	3.75040(10)	3.8389(2)	3.7598(11)
<i>b</i> /Å	15.5185(6)	7.3447(4)	6.954(2)
<i>c</i> /Å	10.6904(4)	22.7544(13)	12.649(4)
α /deg	90	90	90
β /deg	93.351(2)	90	93.678(18)
γ /deg	90	90	90
<i>V</i> /Å ³	621.12(4)	641.57(6)	330.04(17)
<i>Z</i>	4	4	2
<i>F</i> (000)	272	272	136
<i>D</i> _{calc} (g cm ^{−3})	1.402	1.358	1.320
μ (mm ^{−1})	0.095	0.092	0.089
abs correction	multiscan	multiscan	multiscan
<i>T</i> _{min}	0.951	0.934	0.958
<i>T</i> _{max}	0.964	0.986	0.972
2 θ _{max}	70.98	56.44	50.00
no. of reflns collected	17207	6393	2913
no. of unique reflns	2805	1566	2913
no. of obsd reflns	2607	1537	2607
<i>R</i> _{int}	0.0284	0.0334	0.0344
no. of para	91	111	128
no. of restraints	0	0	133
<i>R</i> ₁ [<i>I</i> > 2 σ (<i>I</i>)]	0.0485	0.0341	0.0321
<i>wR</i> ₂ [<i>I</i> > 2 σ (<i>I</i>)]	0.1228	0.0894	0.0834
<i>R</i> ₁ (all data)	0.0524	0.0348	0.0362
<i>wR</i> ₂ (all data)	0.1251	0.0899	0.0875
goodness-of-fit	1.139	1.112	1.063
$\Delta\rho_{\text{max}}, \Delta\rho_{\text{min}}$ (e Å ^{−3})	+0.56, −0.32	+0.27, −0.16	+0.12, −0.14

Table 2. Geometrical Parameters of Intermolecular Interactions in Compounds 2-, 3-, and 4-Cyanobenzaldehyde^a

	D–H...A	D–H (Å)	H...A (Å)	D...A (Å)	D–H...A/ α (deg)
2-cyanobenzaldehyde	C4–H4...O1	0.978 (15)	2.532 (16)	3.4968 (10)	168.9 (12)
	C5–H5...O1	0.95	2.675 (16)	3.3490 (10)	125
	C3–H3...N1	0.969 (14)	2.600 (14)	3.5047 (11)	155.6 (12)
	C6–H6...N1	0.973 (15)	2.611 (15)	3.5081 (11)	153.4 (12)
	Cg1...Cg1		3.7504 (5)		0
3-cyanobenzaldehyde	C4–H4...O1	0.947 (16)	2.394 (17)	3.2807 (16)	155.8 (14)
	C5–H5...O1	0.95	2.61	3.3471 (15)	133
	C2–H2...N1	0.988 (14)	2.568 (15)	3.4831 (16)	154.0 (12)
	C6–H6...N1	0.95	2.64	3.508	152
	Cg1...Cg1		3.8390 (7)		0
4-cyanobenzaldehyde	C3–H3...O1	0.95	2.51	3.341(9)	146
	C5–H5...O1	0.95	2.637	3.519	155
	C6–H6...N1	0.95	2.52	3.378(6)	151
	Cg1...Cg1		3.7599 (17)		0

^aCg1–ring centroid of C1–C6, Cg1...Cg1 is the π stacking interaction, α is the dihedral angle between the planes of benzene ring.

To optimize the structures with higher levels of accuracy, some of the convergence parameters have been changed. Five parameters defined by the keyword TOLINTEG control the accuracy of the evaluation of Coulomb and exchange series, which were set to [8 8 8 8 16] for all calculations.⁸ Shrinking factor, defining sampling of *k*-points is used as (8, 8), and the SCF convergence was set to 10^{−8} hartree for optimization and 10^{−11} hartree for normal mode calculations.

5. RESULTS AND DISCUSSIONS

Bond lengths and bond angles of 2-cyanobenzaldehyde from XRD analysis are compared with the DFT simulation results through RMSD values, which are given in Table 4.

The numbers in the parentheses of the XRD results indicate the uncertainty in the last digits. All simulation values match very well with that of X-ray diffraction results,

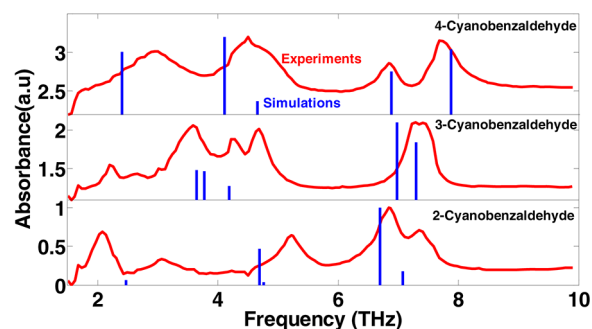


Figure 4. THz absorption spectra of 2, 3 and 4-cyanobenzaldehyde compared with the single molecule simulation results obtained from Gaussian09 software.

with RMSD values of 0.0003 Å for bond lengths and 0.3523° for bond angles.

The simulation results from CRYSTAL14 are compared with the experimental results, as shown in Figure 6. Compared to single molecule simulations using Gaussian09, the crystal simulations are able to accurately predict resonances arising from both intermolecular and intramolecular vibrations. Detailed analysis of the exact mode of vibrations obtained from DFT simulation results shows that the resonances below 3 THz are mostly due to intermolecular vibrations. Because these resonances are absent in single molecule Gaussian simulations, it can be further confirmed that the low frequency resonances (<3 THz) are due to intermolecular vibrational modes only. Resonances from 3 to 10 THz are mainly due to intramolecular vibrations caused by wagging/twisting of the terminal –CHO and –CN groups.

The vibrational spectra show that there are broadly five sets of regions with prominent resonances, located at around 2.1, 3.1, 5.2, 6.8, and 7.4 THz (69, 102, 174, 228, and 245 cm⁻¹). These prominent resonances are considered here for the comparison purposes. Further analysis into the mode of vibration shows that

the absorption band near 2.1 THz is due to in-plane bending. The reason behind the peak at around 3.1 THz has not been ascertained as there are two prominent peaks present: 2.8 and 3.6 THz in the simulation results. Further analysis is required to properly resolve this peak. The resonance at 2.8 THz is mainly due to out-of-plane bending intermolecular vibrations whereas the peak at 3.6 THz is an intramolecular vibration, which is mainly an out-of-plane bending mode due to –CHO twisting and –CN wagging. The reasons behind these resonances are summarized in Table 5.

From Table 5, it can be seen that simulation of full crystal structure provides a good agreement with the experimental resonances yielding a RMSD value of 0.22 THz. The experimental resonance frequency 3.1 THz has been compared with 2.8 THz for RMSD calculation.

Similarly, the bond lengths and bond angles of 3-cyanobenzaldehyde have also been compared with that of XRD values and their corresponding RMSD values are given in Table 6.

The experimental and DFT simulated (CRYSTAL14) spectra of 3-cyanobenzaldehyde are given in Figure 7. From Figure 7, three sets of frequency bands are observed in 3-cyanobenzaldehyde THz spectra, which are around 2, 4, and 7 THz. The peak at 2.2 THz is mainly dominated by intermolecular vibration due to in-plane stretching of C–H...N and C–H...O hydrogen bond. The vibrational modes observed at 2.6 THz and 3 THz are also intermolecular vibrations originating due to out-of plane and in-plane bending of the aromatic rings, respectively. There are three consecutive peaks observed around the 4 THz band, which are 3.6, 4.2, and 4.7 THz. The peak at 3.6 THz is mainly dominated by out-of-plane bending whereas the peaks at 4.2 and 4.7 THz are mainly in-plane bending due to –CN rocking. Table 7 describes the reason behind the resonances up to 10 THz.

In Table 7, it has been shown that the lower THz frequencies are due to intermolecular hydrogen bonding interactions whereas resonances at higher frequencies (up to 10 THz) are

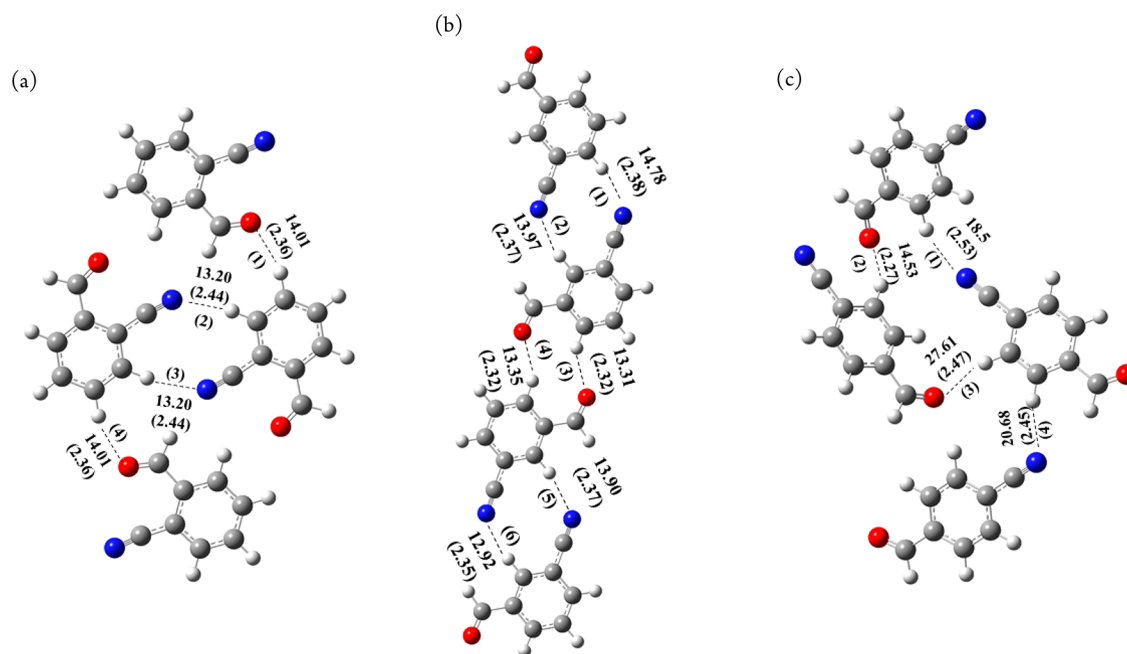


Figure 5. Compliance constants and the corresponding interatomic distances (in brackets) of (a) 2-cyanobenzaldehyde, (b) 3-cyanobenzaldehyde, and (c) 4-cyanobenzaldehyde isomers given in Å/mdyne and Å, respectively.

Table 3. Comparison of Compliance Constants of Various Hydrogen Bonds of Cyanobenzaldehyde Isomers of 2-Cyanobenzaldehyde

2-cyanobenzaldehyde		3-cyanobenzaldehyde		4-cyanobenzaldehyde	
bond	compliance constant (Å/mdyne)	bond	compliance constant (Å/mdyne)	bond	compliance constant (Å/mdyne)
C–H...O (1)	14.01	C–H...N (1)	14.78	C–H...N (1)	18.50
C–H...N (2)	13.20	C–H...N (2)	13.97	C–H...O (2)	14.53
C–H...N (3)	13.20	C–H...O (3)	13.31	C–H...O (3)	27.61
C–H...O (4)	14.01	C–H...O (4)	13.35	C–H...N (4)	20.68
		C–H...N (5)	13.90		
		C–H...N (6)	12.92		

Table 4. Comparison of XRD and Theoretical Bond Lengths (Å) and Bond Angles (deg) of 2-Cyanobenzaldehyde and RMSD Values

bond length	XRD results	simulations	bond angle	XRD results	simulations
C1–C2	1.4116(11)	1.4116	C1–C2–C3	120.15(7)	120.12
C2–C3	1.3954(11)	1.3958	C2–C3–C4	119.84(7)	119.84
C3–C4	1.3953(11)	1.3947	C3–C4–C5	120.24(7)	120.29
C4–C5	1.3903(12)	1.3904	C4–C5–C6	120.03(7)	119.98
C5–C6	1.3927(11)	1.3928	C5–C6–C1	120.64(7)	120.66
C6–C1	1.3932(11)	1.3934	C6–C1–C2	119.10(7)	119.11
C1–C7	1.4806(11)	1.4808	C2–C8–N1	174.47(8)	173.477
C8–N1	1.1542(10)	1.1546	C1–C7–O1	124.52(7)	124.497
C2–C8	1.4405(11)	1.4399	RMSD		0.3523
C7–O1	1.2152(10)	1.2151			
RMSD		0.0003			

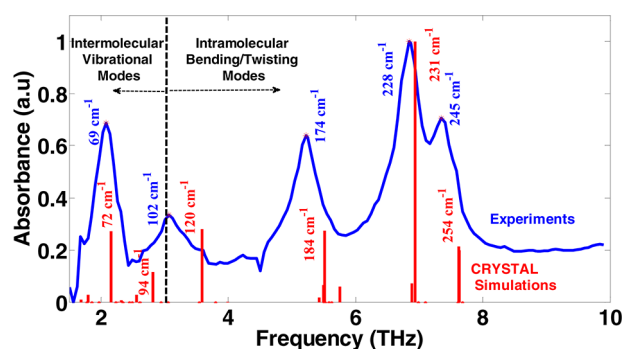


Figure 6. THz absorption spectra of 2-cyanobenzaldehyde and the simulation results obtained from CRYSTAL14 software package.

due to intramolecular in-plane/out-of plane bending of the rings with wagging/twisting of the terminal –CHO and –CN groups.

Similar analysis has been done for 4-cyanobenzaldehyde. From Table 8, comparison of bond lengths and bond angles obtained from XRD analysis and DFT simulation results shows RMSD values of 0.0008 Å for bond length and 0.0422° for bond angle.

THz spectra of 4-cyanobenzaldehyde with its DFT simulation results is given in Figure 8. From this figure, it can be observed that the simulation results match fairly well with that of the experimental spectra.

Figure 8 shows that there is a resonance at around 2.4 THz in the simulation spectra (due to out-of-plane intermolecular vibrations), which is not resolved properly in the experimental spectra. There are four prominent absorption frequency regions observed around 3, 4, 7, and 8 THz (100, 150, 228, and 257 cm^{−1}) in the case of 4-cyanobenzaldehyde. Table 9 describes the assignment of vibrational modes at these frequencies. The low RMSD values obtained from the comparison of experimental and simulation results confirm that the match is fairly well for all the isomers.

6. COMPARISON OF 2-, 3-, AND 4-CYANO BENZALDEHYDE

The studies are aimed toward understanding the possible reasons behind the variation in the spectra as the relative position of –CN group with respect to aldehyde group (–CHO) changes in cyanobenzaldehyde isomers. The resonances in the spectra arise due to intramolecular or intermolecular vibrational modes as revealed by the DFT simulations. However, the lattice

Table 5. Comparison of Experimental and Simulated Resonances of 2-Cyanobenzaldehyde and the Modes of Vibrations

experimental resonances (THz)	crystal simulations (THz)	vibrational assignment
2.1	2.2	in-plane vibrations of aromatic rings due to C–H...N and C–H...O hydrogen bond intermolecular vibrations
3.1	2.8	out-of plane bending of the rings due to intermolecular vibrations of the C–H...N and C–H...O hydrogen bonds
	3.6	out-of plane bending of aromatic rings due to –CHO twisting and –CN wagging
5.2	5.5	out-of-plane bending of the rings due to –CHO and –CN wagging
6.8	6.9	in-plane vibrations of the aromatic rings due to rocking motion of –CHO and –CN group
7.4	7.6	out-of-plane bending of the aromatic rings due to –CH oscillations of the –CHO group
RMSD	0.22	

Table 6. Comparison of XRD and Theoretical Bond Lengths (Å) and Bond Angles (deg) of 3-Cyanobenzaldehyde and Their RMSD Values

bond length	XRD results	simulations	bond angle	XRD results	simulations
C1–C2	1.3954(15)	1.3953	C1–C2–C3	118.90(10)	118.90
C2–C3	1.3962(17)	1.3962	C2–C3–C4	121.05(10)	121.05
C3–C4	1.3983(16)	1.3985	C3–C4–C5	119.42(11)	119.41
C4–C5	1.3961(16)	1.3960	C4–C5–C6	120.07(10)	120.07
C5–C6	1.3884(16)	1.3884	C5–C6–C1	120.18(11)	120.18
C6–C1	1.4007(16)	1.4007	C6–C1–C2	120.38(11)	120.37
C1–C8	1.4832(16)	1.4830	C3–C7–N1	178.81(13)	178.81
C7–C3	1.4488(16)	1.4488	C1–C8–O1	123.37(11)	123.37
C7–N1	1.1457(16)	1.1457	RMSD		0.005
C8–O1	1.2118(15)	1.2118			
RMSD		0.0001			

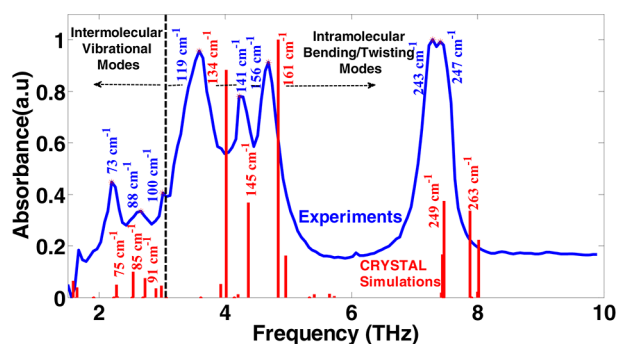


Figure 7. THz absorption spectra of 3-cyanobenzaldehyde and the simulation results obtained from CRYSTAL14 software package.

structures of all the three isomers are also different. Hence, it is not straightforward to compare the mode of vibrations of the isomers. Nevertheless, generic observations can be made regarding variation in the THz resonances of the three isomers.

The simulation results show that there are four sets of frequency bands in the THz spectrum for all the three isomers. These are compared and discussed below:

- (1) Frequency region below 3 THz: In the case of 2-cyanobenzaldehyde, there is a peak at 2.2 THz, which is due to in-plane stretching of C–H...N and C–H...O hydrogen bond formed in the intermolecular interaction. The same mode of vibration is observed for 3-cyanobenzaldehyde at 2.3 THz, which is not clearly resolved in the experimental spectra of 4-cyanobenzaldehyde. Similarly, there is another intermolecular out-of

plane vibration at 2.8 THz for 2-cyanobenzaldehyde and at 2.5 THz for 3-cyanobenzaldehyde.

- (2) The second set of peaks lie between 3 and 4 THz: in the case of 2-cyanobenzaldehyde, there is a peak around 3.6 THz, which is the out-of-plane intramolecular vibration due to –CHO twisting and –CN wagging. The same mode of vibration is observed at 4 THz for 3-cyanobenzaldehyde and a wide peak around 3 THz in the case of 4-cyanobenzaldehyde.
- (3) The third set of modes of vibration is in-plane bending due to –CHO and –CN rocking, which is observed at 6.9 THz for 2-cyanobenzaldehyde, at 7.4 THz for 3-cyanobenzaldehyde, and at 6.9 THz in the case of 4-cyanobenzaldehyde. Because single molecule simulation results match well at higher frequencies (>5 THz), the shift in frequency in this mode can be explained in terms of effective force constant (k_{eff}) and effective reduced mass (μ_{eff}) as given in (2).

$$f = \frac{1}{2\pi} \sqrt{\frac{k_{\text{eff}}}{\mu_{\text{eff}}}} \quad (2)$$

Table 10 shows the effective force constant and effective reduced mass for each vibration at higher frequencies (>5 THz) of the three isomers. Though the exact frequencies do not match, the trend can be explained using Gaussian simulation results.

From the above table, it is clear that the resonance frequency of 3-cyanobenzaldehyde is higher than that of 2-cyanobenzaldehyde due to its lower reduced mass.

- (4) The fourth set of frequencies (>7.5 THz): These are mainly out-of-plane bending modes due to wagging of –CH of –CHO group, observed at 7.6, 7.9, and 8.1 THz for 2-,

Table 7. Comparison of Experimental and Simulated Resonances of 3-Cyanobenzaldehyde and the Modes of Vibrations at These Frequencies

experimental resonances (THz)	crystal simulations (THz)	vibrational assignment
2.2	2.3	in-plane vibrations of aromatic rings due to C–H...N and C–H...O bond intermolecular vibrations
2.6	2.5	out-of-plane bending of the rings primarily due to intermolecular vibrations of C–H...N and C–H...O hydrogen bonds
3	2.7	in-plane vibrations of rings due to intermolecular C–H...N and C–H...O vibrations
3.6	4	out-of-plane bending of rings due to –CHO twisting and –CN wagging
4.2	4.36	in-plane vibration of rings primarily due to –CN rocking
4.7	4.8	in-plane motion due to –CN rocking
7.3	7.4	In-plane vibrations in rings due to –CHO and –CN rocking
7.4	7.9	out-of-plane bending of rings due to –CH oscillations of –CHO
RMSD	0.266	

Table 8. Comparison of XRD and Theoretical Bond Lengths (Å) and Bond Angles (deg) of 4-Cyanobenzaldehyde and the RMSD Values

bond length	XRD results	simulations	bond angle	XRD results	simulations
C1–C2	1.394(5)	1.394	C1–C2–C3	117.2(3)	117.22
C2–C3	1.388(4)	1.387	C2–C3–C4	121.4(3)	121.45
C3–C4	1.347(4)	1.347	C3–C4–C5	120.2(2)	120.16
C4–C5	1.370(4)	1.370	C4–C5–C6	121.7(2)	121.73
C5–C6	1.344(4)	1.344	C5–C6–C1	118.2(3)	118.22
C6–C1	1.402(4)	1.402	C6–C1–C2	121.2(2)	121.14
C1–C7	1.594(9)	1.593	C4–C8–N1	144.4(8)	144.33
C4–C8	1.488(11)	1.489	C1–C7–O1	127.3(8)	127.3
C8–N1	1.031(9)	1.029	RMSD		0.0422
C7–O1	1.111(8)	1.111			
RMSD		0.0008			

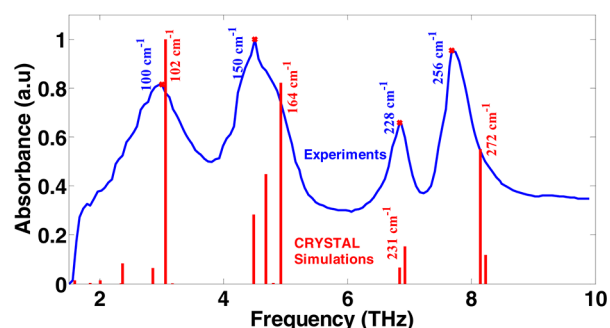


Figure 8. THz absorption spectra of 4-cyanobenzaldehyde and the simulation results obtained from CRYSTAL14 software package.

Table 9. Comparison of Experimental and Simulated Resonances of 4-Cyanobenzaldehyde and the Modes of Vibrations

experimental resonances (THz)	crystal simulations (THz)	vibrational assignment
3	3	out-of-plane bending of rings due to twisting of CHO and –CN wagging (Intramolecular)
4.5	4.9	in-plane bending of rings due to –CHO wagging and –CN rocking
6.8	6.9	in-plane vibrations of the rings due to rocking of –CHO and –CN
7.9	8.1	out-of-plane bending of the rings primarily due to –CH wagging of the –CHO group
RMSD	0.23	

Table 10. Resonance Frequency (f) (Gaussian09 Simulations Using the B3LYP Density Functional with the 6-31G(d,p) Basis Set) Shift Due to the Effective Reduced Mass (μ_{eff}) and Effective Force Constant (k_{eff}) of the Cyanobenzaldehyde Isomers

2- cyanobenzaldehyde			3-cyanobenzaldehyde			4-cyanobenzaldehyde		
f_i THz	k_{eff} N/m	μ_{eff} amu	f_i THz	k_{eff} N/m	μ_{eff} amu	f_i THz	k_{eff} N/m	μ_{eff} amu
6.7	0.2	7.1	7.0	0.2	6.5	6.9	0.2	6.3
7.1	0.1	2.7	7.3	0.1	2.6	7.9	0.13	3.4

3-, and 4-cyanobenzaldehyde, respectively. From Table 10, 3-cyanobenzaldehyde has a higher resonant frequency compared to 2-cyanobenzaldehyde due to its lower reduced mass and for 4-cyanobenzaldehyde the frequency is shifted to higher value due to its higher force constant and lower reduced mass.

7. CONCLUSION

THz spectra of cyanobenzaldehyde isomers have been studied using solid state DFT simulations in the frequency region between 2 and 10 THz. Room temperature XRD results provide the crystal structures of 2-, 3-, and 4-cyanobenzaldehyde isomers. B3LYP hybrid density functional with 6-31G(d,p) basis sets are utilized for the simulations to assign the THz spectra for both a single molecule and full crystal structures. By carrying out both single molecule and crystal simulations, we have clearly distinguished intermolecular and intramolecular vibrations. It has been demonstrated that resonances below 3 THz are mainly dominated by intermolecular vibrations mediated by hydrogen bonds whereas the higher resonances are due to intramolecular in-plane/out-of-plane bending vibrations arising due to wagging/twisting of –CHO and –CN terminal groups. THz resonances provide a unique fingerprint of molecules and hence can be used for isomer identification. Understanding the origin of THz resonances can help in designing molecules with multiple and tunable frequencies in THz region, especially below 1 THz.

AUTHOR INFORMATION

Corresponding Author

*B. Pesala. E-mail: balapesala@gmail.com.

Notes

The authors declare no competing financial interest.

ACKNOWLEDGMENTS

The authors of CSIR-CEERI thank Director General, CSIR, and Director and Scientist-in-Charge, CSIR-CEERI Chennai, for their invaluable support throughout the research work. Part of the research work has been carried out with the equipment of CSIR Innovation Complex for which authors thank the Director, CSIR-SERC. The authors acknowledge the financial support for this work through CSIR network project CSC-0128 (FUTURE). Co-author Shaumik Ray thanks CSIR for financial support.

REFERENCES

- (1) Zeitle, J. Axel; Taday, Philip F.; Newnham, David A.; Pepper, Michael; Gordon, Keith C.; Rades, Thomas. Terahertz pulsed spectroscopy and imaging in the pharmaceutical setting – a review. *J. Pharm. Pharmacol.* **2007**, *59*, 209–223.
- (2) Davies, Giles; Burnett, Andrew D.; Fan, Wenhui; Linfield, Edmund H.; Cunningham, John E. Terahertz spectroscopy of explosives and drugs. *Mater. Today* **2008**, *11*, 18.
- (3) Globus, Tatiana; Moyer, Aaron M.; Gelmont, Boris; Khromova, Tatyana; Lvovska, Maryna I.; Sizov, Igor; Ferrance, Jerome. Highly

Resolved Sub-Terahertz Vibrational Spectroscopy of Biological Macromolecules and Cells. *IEEE Sensors J.* **2013**, *13* (1), 72–79.

(4) Walther, M.; Plochcka, P.; Fischer, B.; Helm, H.; Jepsen, P. Uhd. *Collective Vibrational Modes In Biological Molecules Investigated by Terahertz Time-Domain Spectroscopy*; Wiley Interscience: New York, 2002; DOI: 10.1002/Bip.10106.

(5) Amalanathan, M.; Hubert Joe, I.; Prabhu, S. S. Charge Transfer Interaction and Terahertz studies of a Nonlinear Optical Material L-Glutamine Picrate: A DFT study. *J. Phys. Chem. A* **2010**, *114*, 13055–13064.

(6) King, Matthew D.; Ouellette, Wayne; Korter, Timothy M. Noncovalent Interactions in Paired DNA Nucleobases Investigated by Terahertz Spectroscopy and Solid-State Density Functional Theory. *J. Phys. Chem. A* **2011**, *115*, 9467–9478.

(7) Castro-Camus, E.; Johnston, M. B. Conformational changes of proactive yellow protein monitored by terahertz spectroscopy. *Chem. Phys. Lett.* **2008**, *455*, 289–292.

(8) Oppenheim, Keith C.; Korter, Timothy M.; Melinger, Joseph S.; Grischkowsky, Daniel Solid-State Density Functional Theory Investigation of the Terahertz Spectra of the Structural Isomers 1, 2-Dicyanobenzene and 1, 3-Dicyanobenzene. *J. Phys. Chem. A* **2010**, *114*, 12513–12521.

(9) Jiang, Ye; Zhou, Fengshan; Wen, Xiaodong; Yang, Limin; Zhao, Guozhong; Wang, He; Haiyan, Wang; Yanjun, Zhai; Jinguang, Wu; Kexin, Liu; Jia'er, Chen. Terahertz Absorption Spectroscopy of Benzamide, Acrylamide, Caprolactam, Salicylamide and Sulfanilamide in the Solid State. *J. Spectrosc.* **2014**, *2014*, 732802.

(10) Frisch, M. J.; et al. *Gaussian 09*, Revision D.01; Gaussian, Inc.: Wallingford, CT, 2009.

(11) Dovesi, R.; Orlando, R.; Erba, A.; Zicovich-Wilson, C. M.; Civalieri, B.; Casassa, S.; Maschio, L.; Ferrabone, M.; De La Pierre, M.; D'Arco, P.; Noel, Y.; Causa, M.; Rerat, M.; Kritman, B. CRYSTAL14: A program for the ab initio investigation of crystalline solids. *Int. J. Quantum Chem.* **2014**, *114*, 1287.

(12) Dovesi, R.; Saunders, V. R.; Roetti, C.; Orlando, R.; Zicovich-Wilson, C. M.; Pascale, F.; Civalieri, B.; Doll, K.; Harrison, N. M.; Bush, I. J.; D'Arco, P.; Llunell, M.; Causa, M.; Noel, Y. *CRYSTAL 14 User's Manual*; University of Torino: Torino, 2014.

(13) Ray, Shaumik; Dash, Jyotirmayee; Nallappan, Kathirvel; Kaware, Vaibhav; Basutkar, Nitin; Ambade, Ashootosh; Joshi, Kavita; Pesala, Bala. Design and Engineering of Organic Molecules for Customizable Terahertz Tags. *Proc. SPIE* **2014**, *8985*, 89850P–89850P-8.

(14) APEX2, SAINT, and SADABS; Bruker AXS Inc.: Madison, WI, USA, Bruker, 2006.

(15) Sheldrick, G. M. A Short History of SHELX. *Acta Crystallogr., Sect. A: Found. Crystallogr.* **2008**, *64*, 112–122.

(16) Fisher, B. M.; Walther, M.; Uhd Jepsen, P. Far-infrared vibrational modes of DNA components studied by terahertz time-domain spectroscopy. *Phys. Med. Biol.* **2002**, *47*, 3807–3814.

(17) Kleine-Ostmann, Thomas; Wilk, Rafal; Rutz, Frank; Koch, Martin; Niemann, Henning; Guttler, Bernd; Brandhorst, Kai; Grunenberg, Jörg Probing Noncovalent Interactions in Biomolecular Crystals with Terahertz Spectroscopy. *ChemPhysChem* **2008**, *9*, 544–547.

(18) Brandhorst, Kai; Grunenberg, Jörg. How Strong is it? The interpretation of force and compliance constants as bond strength descriptors. *Chem. Soc. Rev.* **2008**, *37*, 1558–1567.